Light and dark biocidal activity of cationic poly(arylene ethynylene) conjugated polyelectrolytes

ARTICLE *in* PHOTOCHEMICAL AND PHOTOBIOLOGICAL SCIENCES · AUGUST 2009

Impact Factor: 2.27 · DOI: 10.1039/b902646k · Source: PubMed

8 AUTHORS, INCLUDING:

Liping Ding
Shaanxi Normal University
50 PUBLICATIONS **954** CITATIONS
SEE PROFILE

Eunkyung Ji
University of Florida
16 PUBLICATIONS **336** CITATIONS
SEE PROFILE

Linnea K Ista
University of New Mexico
53 PUBLICATIONS **1,813** CITATIONS
SEE PROFILE

Kirk S Schanze
University of Florida
325 PUBLICATIONS **11,321** CITATIONS
SEE PROFILE

This article is published as part of a themed issue of ***Photochemical & Photobiological Sciences*** in honour of

Esther Oliveros

Guest edited by **Marie-Thérèse Maurette** and **Guillermo Orellana**

Published in **issue 7, 2009**

Other articles in this issue include:

Light and dark biocidal activity of cationic poly(arylene ethynylene) conjugated polyelectrolytes†

Thomas S. Corbitt,[a] Liping Ding,[a,c] Eunkyung Ji,[b] Linnea K. Ista,[a] Katsu Ogawa,[b] Gabriel P. Lopez,[a] Kirk S. Schanze[b] and David G. Whitten*[a]

Received 9th February 2009, Accepted 26th May 2009
First published as an Advance Article on the web 8th June 2009
DOI: 10.1039/b902646k

In this paper we report a study of cationic poly(arylene ethynylene) conjugated polyelectrolytes. The objective of the study was to compare the behavior of a polymer where a thiophene has replaced a phenyl ring in poly(phenylene ethynylene) polycations (PPE) previously investigated. Properties of solution phase and physisorbed suspensions of the polymer on microspheres were investigated. The photophysical properties of the polymer are evaluated and used to understand the striking differences in biocidal activity compared to the PPE polymers previously examined. The principal findings are that the thiophene polymer has remarkable dark biocidal activity against *Pseudomonas aeruginosa* strain PAO1 but very little light-activated activity. The low light-activated biocidal activity of the thiophene polymer is attributed to a highly aggregated state of the polymer in aqueous solutions and on microspheres as a physisorbed coating. This results in low triplet yields and a very poor sensitization of singlet oxygen and other reactive oxygen intermediates. The highly effective dark biocidal activity of the thiophene-containing polymers is attributed to its high lipophilicity and the presence of accessible quaternary ammonium groups. The difference in behavior among the polymers compared provides insights into the mechanism of the dark process and indicates that aggregation of polymer can reduce light activated biocidal activity by suppressing singlet oxygen generation.

1. Introduction

Increasingly, cationic polymers have taken their place among various classes of materials effective as long-lasting antimicrobials and biocides.[1] Among the advantages of such polymers over monomeric and small organic biocides are lower residual toxicity, increased lifetimes and increased specificity and potency.[1] Cationic biocidal polymers are thought to function by associating with negatively charged bacteria, permeating the bacterial cell wall and physically disrupting the underlying cell membrane.[1,2–6] The physical mechanism resulting in membrane disruption has been suggested to involve association of the cationic groups with the phospholipid bilayer membrane followed by an ion exchange process in which the organic cations exchange with inorganic cations resulting in a destabilization of the membrane and subsequent pore formation or collapse.[6,7]

Conjugated polyelectrolytes (CPE) have gained significant attention due to their unique materials and photophysical properties.[8–13] In particular, CPEs are soluble in water and polar organic solvents, and the presence of the ionic solubilizing groups allows the polymers to interact strongly with ions in solution and with charged planar or colloid surfaces. Due to their relatively high carbon atom to ionic group ratio, CPEs are polymer amphiphiles, and they self-assemble into nanoscale aggregates in aqueous solution and they adsorb strongly to charged substrates forming films that can be tailored on the nanoscale. In addition to these interesting and useful materials properties, CPEs also have favorable photophysical properties such as efficient light harvesting ability (large absorption coefficients), rapid singlet exciton diffusion along the conjugated backbone, high fluorescence quantum yields, and they display the amplified fluorescence quenching effect.[14–17] Such desirable characteristics of CPEs have led to their use a variety of applications including chemo- and bio-sensors,[8,18] photovoltaic devices,[19,20] and light-activated antimicrobial materials.[21,22]

In work reported earlier we found that cationic CPE **1** and **2** show little biocidal activity against *Cobetia marina* or *Pseudomonas aeruginosa* strain PAO1 (PAO1) when microspheres with physisorbed or surface grafted conjugated polyelectrolytes are mixed with bacterial suspensions in the dark for short periods of time 15 min–1 h.[23] Over prolonged incubation in the dark there is a slow killing of the bacteria. However, when the same suspensions are irradiated with visible light in the presence of oxygen, there is a relatively rapid light-activated biocidal activity that likely involves interfacial generation of singlet oxygen and perhaps subsequent formation of more corrosive reactive oxygen species.[23]

In the present paper we report a study of a third CPE in this series, **3**, that contains a thiophene ring replacing one of the phenyl rings in the poly(phenylene ethynylene) (PPE) repeat unit. This polymer exhibits somewhat different photophysical behavior from CPEs **1** and **2**. The new behavior results in dramatically

[a]*Center for Biomedical Engineering and Department of Chemical and Nuclear Engineering, University of New Mexico, Albuquerque, NM, 87131-0001, USA*
[b]*Department of Chemistry, University of Florida, Gainesville, FL, 32611-7200, USA*
[c]*School of Chemistry and Materials Science, Shaanxi Normal University, Xi'an, 710062, P. R. China*
† This article was published as part of the themed issue in honour of Esther Oliveros.

reduced light activated biocidal activity; we find however that **3** shows remarkable dark biocidal activity. This difference in behavior provides insights into the mechanism of the dark process and the way dark and light-activated biocidal activity may be tuned.

2. Experimental

2.1 Chemicals

Polymer **2**,[24] polymer **3**[25] and 1,3-cyclohexadiene 1,4-diethanoate (CHDDE)[26] were synthesized according to literature procedures. 2′-Acetonaphthone and 5,10,15,20-tetrakis(4-sulfonatophenyl)porphyrin (TPPS) were purchased from J. T. Baker and Sigma-Aldrich Chemical Company, respectively. Non-porous borosilicate glass microspheres (5 μm diameter) were purchased in dry powder form from Duke Scientific (Palo Alto, CA). 1,2-Dioleoyl-sn-glycero-3-[phospho-rac-(1-glycerol)] (sodium salt) (DOPG) was purchased from Avanti Polar Lipids (Alabaster, AL). Phosphate buffer saline (PBS) was prepared according to a standard procedure and has a pH value of 7.4. Milli-Q water (18.2 MΩ cm^{-1}) was used to prepare all aqueous solutions.

2.2 Photophysical characterization methods

UV-vis absorption spectra were obtained with samples contained in 1 cm quartz cuvettes on a Varian Cary 100 spectrometer. Steady state fluorescence emission spectra were recorded on a PTI (Photon Technology International) fluorometer. Transient absorption spectra were collected using laser systems that are described elsewhere.[27,28] Polymer solutions were prepared in methanol or water and then purged with argon for 1 h before making transient absorption spectroscopy measurements. Singlet oxygen quantum yields were determined in water or methanol according to the procedures described elsewhere.[23]

2.3 Preparation of PPE-coated glass microspheres (Si-PPE)

Two different cationic CPEs, **2** and **3** were used to adsorb on the surface of borosilicate glass microspheres which are slightly negatively charged. A given amount of microspheres (50 mg, *ca.* 3.0×10^8 spheres) were suspended in 1 mL of water first and mixed for a few minutes by using a vortex mixer. Then, the amount of PPE needed to provide 1.2 monolayers of CPE per sphere was calculated according to the method reported elsewhere[29] and added to the microsphere suspension. The whole system was mixed strongly using a vortex mixer for 30 min. Finally, the suspension was centrifuged, and the supernatant was decanted and discarded. The resulting PPE-coated glass microspheres (Si-**2** and Si-**3**) were resuspended in 1 mL of water and used as stock solution after 10 times of rinsing cycles—centrifuge, decant, discard, and resuspend. There was no free polymer in the supernatant as evidenced by fluorescence measurement.

2.4 Preparation of DOPG liposomes and lipobeads

DOPG liposomes were prepared according to the following procedure: 1 mL of 2 mM solution of DOPG in chloroform was first dried under vacuum overnight. The dried lipids were then hydrated by 1 mL of PBS buffer and mixed for 5–10 min, and the resulting DOPG liposome suspensions were extruded to optical clarity by using a mini-extruder (Avanti Polar Lipids, Alabaster, AL) and extruding through an 0.8 μm polycarbonate membrane filter 11 times. Lipobeads were prepared by adding 100 μL of each stock Si-PPE suspension to 1 mL of DOPG liposome prepared as described above and mixed at r.t. using a vortex mixer for 30 min. The resulting lipobeads, Si-**2**-DOPG and Si-**3**-DOPG, were centrifuged and the supernatant containing extra liposome was decanted and discarded. The cycle—resuspend, centrifuge, decant and discard—was repeated four additional times to make sure there was no extra DOPG in the supernatant, and the lipobeads were resuspended in 1 mL of PBS.

2.5 Preparation of bacterial samples

The Gram negative bacterium *P. aeruginosa*, strain PAO1, (a kind gift acquired from Dr Tim Tolker-Nielsen) was stored as frozen stock in nutrient broth (Difco); NB +20% glycerol at −70 °C. Experimental stock cultures were maintained on nutrient agar (NA) slants and were stored at 4 °C for up to 2 weeks. Prior to inoculation into a chemostat, a single colony from a NA slant was inoculated into 50 mL of NB and grown overnight with shaking at 25 °C. A chemostat culture was established by inoculating 3 mL of the overnight culture into citrate minimal medium.[23] The chemostat was maintained at a flow rate of 1.0 mL min^{-1} (dilution rate, 0.12 h^{-1}) with constant stirring. The concentration of the chemostat culture was 10^7 cells mL^{-1}.

2.6 Biocide studies, dead/live assays

Chemostat grown PAO1 was collected by centrifuging 27 mL of culture at 10 000 rpm in an Eppendorf 5415C for 4 min. The pellet was re-suspended in 1 mL 0.85% NaCl solution and repelleted. The wash cycle was repeated 3 times. Bacterial concentrations were normalized using hemocytometer counts. Bacteria were added to polymer-coated particles in aliquots of 200–500 μL, depending on concentration, so that a ratio of ~30 bacteria per bead was achieved. The live control was cells suspended at similar concentrations, but without beads. Polymer-coated microsphere/bacteria samples and live controls were exposed to white light (30 min, Fiber Lite 190 on "high" setting, 1 W cm^{-2} at 1 cm). All samples were gently shaken during this exposure period. A separate control set was kept dark by covering with Al foil.

Dead/live assays were performed using SYTO 60 and SYTOX Green (Molecular Probes, www.invitrogen.com). SYTO 60 is a cell membrane permeant dye with red (~650 nm) fluorescence and used to stain both live and dead cells; SYTOX Green is a green-fluorescent nuclear and chromosome counterstain that is impermeant to live cells but stains the chromatin of dead cells with comprised membranes and emits green (~530 nm) fluorescence, indicating cell death. Upon completion of treatment outlined above, a 1 : 1 ratio of dyes was added to the samples (2 μL mixed dye per mL suspension) and incubated for 15 min in the dark. Bacteria were then examined under a 40× oil objective on a Zeiss LSM 510 Meta confocal laser scanning microscope and the number of live cells (*i.e.* those fluorescing red only) and dead cells (*i.e.* those fluorescing both red and green) compared.

2.7 Data collection

Fluorescence spectra of polymers **2** and **3** mixed with either PAO1 bacteria or DOPG liposome and microspheres coated by these polymers were performed on a SpectroMax M-5 microplate reader (Molecular Devices) using a 96-well plate, where 100 μL of each sample containing either 1.3×10^{-5} M PPE polymers solution or 3.0×10^{6} Si-PPE microspheres was analyzed. The excitation wavelengths for polymer **2** and **3** are 394 nm and 427 nm, respectively. The emission spectra were collected from 430 to 650 nm for polymer **2** and from 460 nm to 700 nm for polymer **3**.

Table 1 Photophysical properties of **2** and **3**

Polymer	Solvent	λ_{max}^{abs}/nm	λ_{max}^{fl}/nm	Φ_{fl}	Φ_{Δ}[e]
3	MeOH	422	475, 502	0.045 (± 0.005)[a]	0.112 (± 0.008)[b]
	H_2O	432	475, 502	0.016 (± 0.002)[a]	0.037 (± 0.001)[b]
2[c]	MeOH	422	441	0.15 (± 0.02)[d]	0.122 (± 0.012)[b]
	H_2O	394	436	0.047 (± 0.005)[d]	0.32 (± 0.039)[b]

[a] Coumarin 30 in MeOH as standard, $\Phi_{fl} = 0.307$ (ref. 32), $\lambda_{ex} = 425$ (MeOH), $\lambda_{ex} = 419$ (H_2O). [b] Oxygen-saturated solution. [c] From ref. 24. [d] Coumarin 1 in EtOH as standard, $\Phi_{fl} = 0.73$ (ref. 33), $\lambda_{ex} = 370$ nm. [e] Quantum yield of singlet oxygen.

3. Results and discussion

3.1 Photophysical properties

The structures of CPEs used in the present work are illustrated in Scheme 1. Polymer **2** and **3** are poly(phenylene ethynylene) (PPE)-based CPEs that feature quaternary ammonium salts on the side chains. CPEs exist in a "molecularly dissolved" state with minimal aggregation in a good solvent, such as methanol. In poor solvent, on the other hand, they exist as aggregates.[16,17] Aggregation of polymer chains results in changes in photophysical behavior of the polymers in solution.[24,30,31] In general, PPE-based CPEs exhibit red-shift and narrowing of absorption spectrum and red-shift and broadening of fluorescence spectrum upon switching from a good solvent to a poor solvent.

As seen in Fig. 1, a methanol solution of polymer **3** exhibits a broad absorption band with λ_{max} at 422 nm. In aqueous solution, the absorption maximum red-shifts to 432 nm and also the absorption coefficient decreases. The emission properties are more dependent on the nature of the solvent. In methanol solution, polymer **3** exhibits a narrow emission band at $\lambda_{max} = 475$ nm with a vibronic band at $\lambda_{max} = 502$ nm. In aqueous solution, the emission band becomes broader and the fluorescence quantum yield ($\Phi_{fl} = 0.016$) is lower than that in methanol ($\Phi_{fl} = 0.045$). Interestingly, the emission maximum is at the same position as in methanol (475 nm) with a shoulder at 502 nm. Such behavior is different from other PPE-based CPEs, which exhibit large red-shifts of emission band in a poor solvent. The lack of a spectral shift for **3** likely is due to the fact that the aggregated state of the polymer has a much lower quantum yield, and therefore its contribution to the total emission spectrum is small. The photophysical properties of **2** were previously studied and reported in the literature.[24] The photophysical data of polymer **2** and **3** are summarized in Table 1.

The triplet excited state plays an important role in singlet-oxygen generation. In previous studies, transient absorption spectroscopy

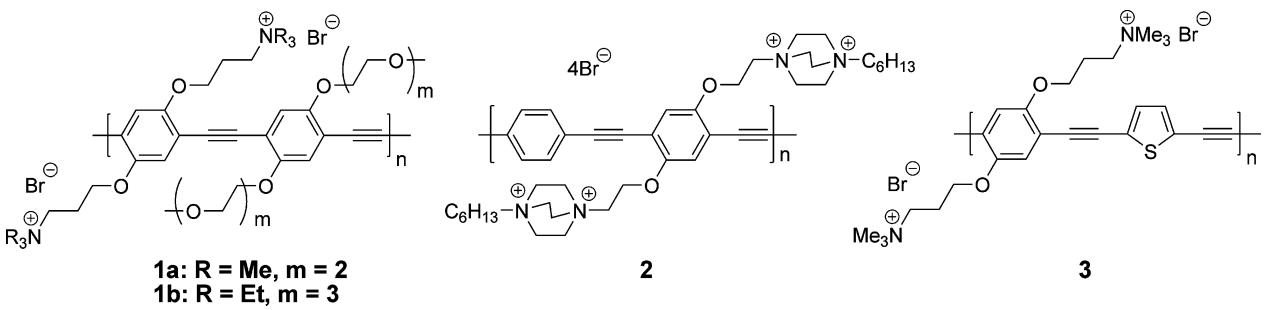

Scheme 1 Structures of cationic conjugated polyelectrolytes.

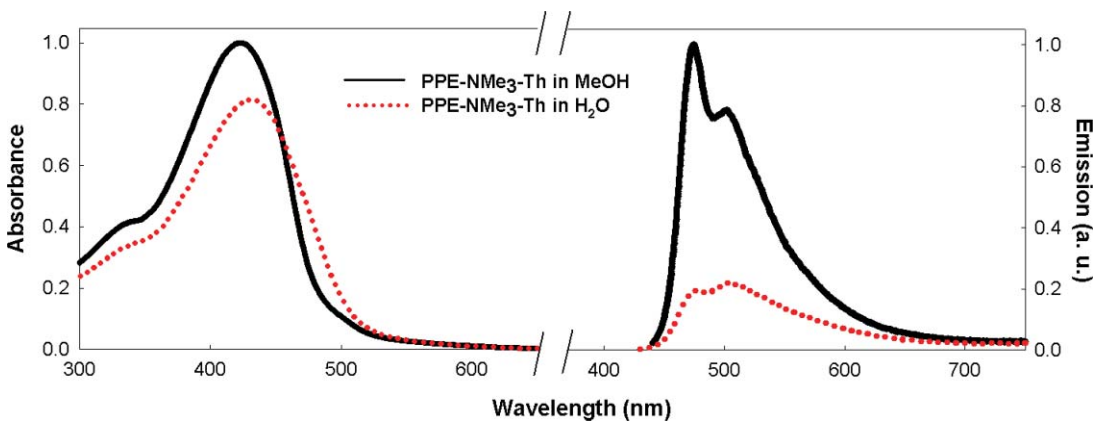

Fig. 1 Absorption and emission spectra of **3** in methanol and aqueous solution. The spectra are normalized according to absorption coefficients (absorption) and relative emission quantum yields (emission).

was utilized to investigate triplet states of non-phosphorescent PPE-based conjugated polymers.[23,34] The presence of the triplet excited state was confirmed by a broad intense transient absorption band centered at λ_{max} ~ 760 nm. As seen in Fig. 2, **3** exhibits a transient absorption band centered at λ_{max} ~ 760 nm quite similar to other PPE-based CPEs. The lifetimes of the transient absorption are 40 (± 10) μs in aqueous solution and 12 (±3) μs in methanol solution. The appearance of the spectra and lifetimes strongly suggest that the transient species is the triplet state of **3**. The lower intensity of the transient absorption in water suggests that the triplet yield is lower in comparison to methanol solution. Such a lower triplet yield in water can be explained by aggregation of the polymer, which quenches the singlet excited state of the polymer. This is consistent with the reduced fluorescence intensity of polymer in water compared to in methanol.

3.2 Microsphere-based biocidal activity studies

A series of experiments to test for biocidal activity were carried out using **3** as a physisorbed coating on 5 μm SiO_2 microspheres. These microspheres were exposed to PAO1 and observed for association and biocidal activity using confocal microscopy. The bacteria attach to the surface-associated polymers in an adsorptive process, likely driven by hydrophobic and electrostatic interactions, analogous to adsorption of polyelectrolytes to an oppositely charged colloidal particle.[21] This process occurs in the dark or light and does not, in itself, result in short term killing of the bacteria although some physical damage (and longer term killing) of the bacteria may occur. This association is reversible to some extent and real time observation of a single particle–bacteria cluster reveals that some bacteria associate briefly and then are released while others appear to be captured irreversibly.

As previously observed,[22,23] and as shown in Fig. 3a and b, clusters of microspheres along with bacteria begin to agglomerate as bacteria are killed, presumably due to the release of microbial agglutinants as the cell membranes are compromised. In solution, these agglomerates tend to be a rough indicator of the antimicrobial activity over time, with samples starting out with fairly monodisperse solutions of coated microspheres to which the bacteria are added. In the samples using **3**, large aggregates with pronounced antimicrobial activity appeared within 15 min of introduction of bacteria. Light-exposed samples tended to have less aggregation and actually showed diminished biocidal action, even with bacteria intimately associated with the coated microspheres (Fig. 3b).

This is in contrast with the behavior of physisorbed **1** and **2**, suspensions of which show some dark and significant light-activated biocidal activity against PAO1 but less agglomeration.[23] Microspheres with physisorbed **1** and **2** also show much stronger fluorescence than physisorbed **3** even when coated at the same density. Interestingly, when microspheres of physisorbed **3** are overcoated with a phospholipid bilayer the fluorescence levels

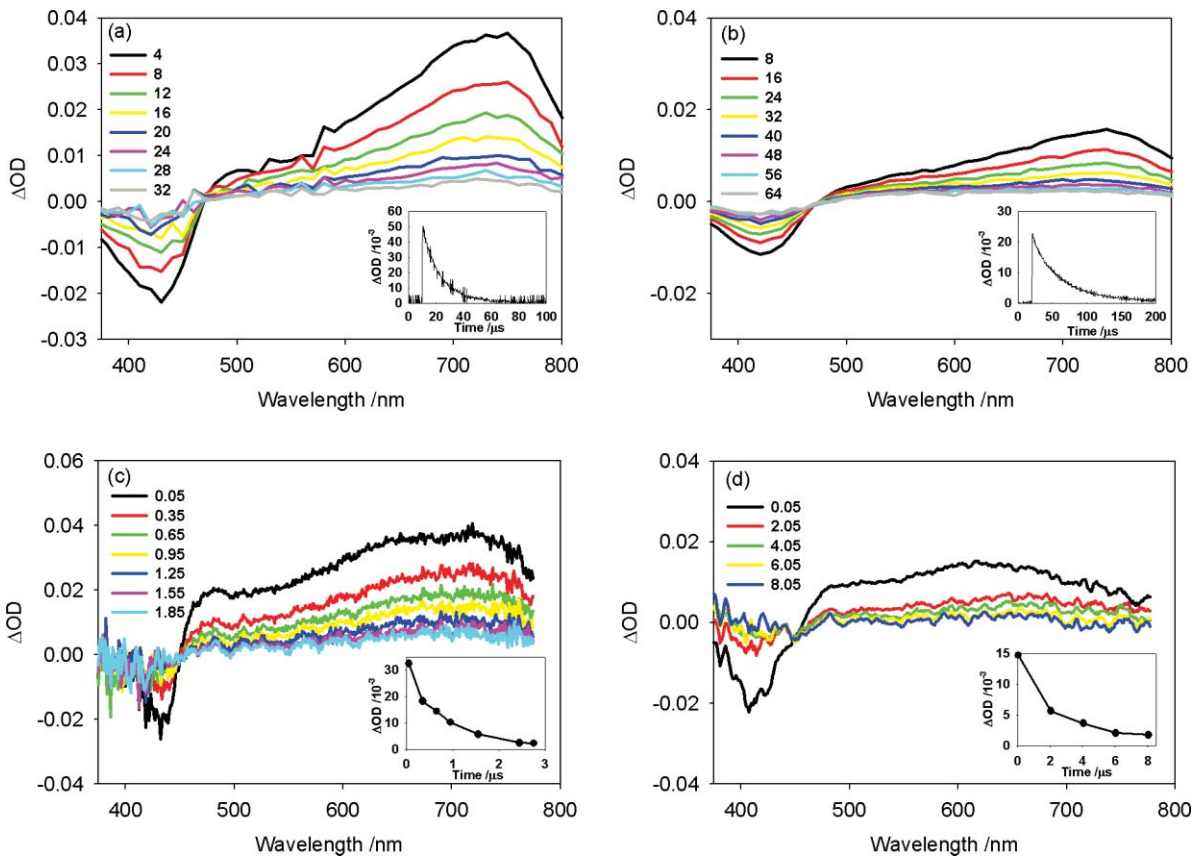

Fig. 2 Transient absorption difference spectra of **2** and **3**. (a) **3** in methanol, (b) **3** in water, (c) **2** in methanol, and (d) **2** in water. Insets: Transient absorption difference decay curves. All experiments were done with solutions having matched OD of 0.7 at 355 nm and excited with the same laser energy at 10 mJ. The spectra in (a) and (b) were obtained on the laser system described in ref. 27, and those in (c) and (d) were obtained on the system described in ref. 28.

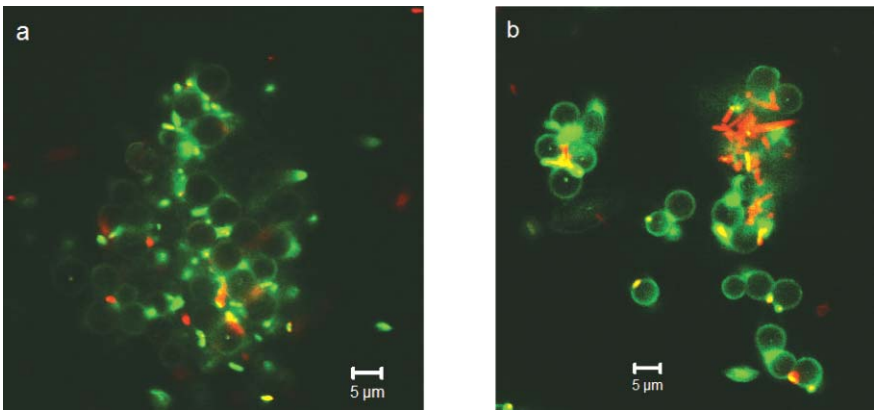

Fig. 3 Comparison of biocidal activity in the dark (a) and light-exposed (b) solutions of **3** physisorbed onto 5 μm glass microspheres. In the images, the live bacteria are red and the dead bacteria are green. The polymer is observed as a very faint green color on the surface of the glass microspheres.

are much stronger.[25] It should be noted that it is very difficult to keep dark suspensions rigorously dark and some irradiation does occur during subsequent confocal fluorescence imaging. Unexposed PAO1 typically remained viable for more than six hours, longer than the total experimental time. For microspheres with physisorbed **3** incubation with PAO1 in the dark for 2 h results in greater than 95 percent killing of the bacteria.

3.3 Biocidal activity of 3 in solution

Addition of polymer solutions to suspensions of PAO1 also results in dark biocidal activity for both **2** and **3**; however there are clear differences in the behaviors of the two polymers as shown in Fig. 4. Treatment of PAO1 with **3** results in clustering of the bacteria and rapid killing as shown in Fig. 4a. In contrast treatment of PAO1 with **2** results in very little agglomeration of the bacteria (Fig. 4b). As will be discussed below we believe this behavior can be attributed to the lipophilic character of polymer **3**.

3.4 Fluorescence studies of polymers 2 and 3 with PAO1

Fluorescence spectra of both polymers **2** and **3** in 0.85% NaCl aqueous solution were measured in the absence and presence of PAO1 bacteria using a plate reader. As the rod-shaped PAO1 we used is *ca.* 2 μm in length and 0.7 μm in diameter, the calculated surface area of per PAO1 is *ca.* 4.7×10^{-12} m^2. According to the literature,[31] the surface area per PPE repeat unit is *ca.* 2.8×10^{-18} m^2. Therefore, about 1.7×10^6 PPE repeat units can be associated on the surface of each PAO1. 10 μL of polymer **2** and **3** stock solutions (1.3 mM in PPE repeat unit) were respectively added to 500 μL of PAO1 solution (*ca.* 2.3×10^8 PAO1). This results in 20 times full coverage of PPE polymers on PAO1 surface. The fluorescence emission spectra of mixtures of polymers with PAO1 as well as control samples without PAO1 are shown in Fig. 5. While mixing with PAO1 resulted in a moderate decrease (30%) in the fluorescence intensity of polymer **2**, the fluorescence intensity for polymer **3** decreased dramatically (~80%) under the same conditions. This result could be attributed to the fact that clusters were formed between PAO1 and polymer **3** and that not many clusters formed between PAO1 with polymer **2**, as shown in Fig. 4. In the clusters, polymer **3** aggregated around PAO1 and resulted in higher local concentration, which could result in an apparent quenching of the polymer fluorescence. Since the polymer **2** was well distributed in the solution in the presence of PAO1 as shown in confocal data, it is reasonable to observe less fluorescence decrease for polymer **2**. These results once again confirmed that the structure difference between polymers **2** and **3** brings different interaction between CPEs and bacteria, and results in different dark biocidal activity.

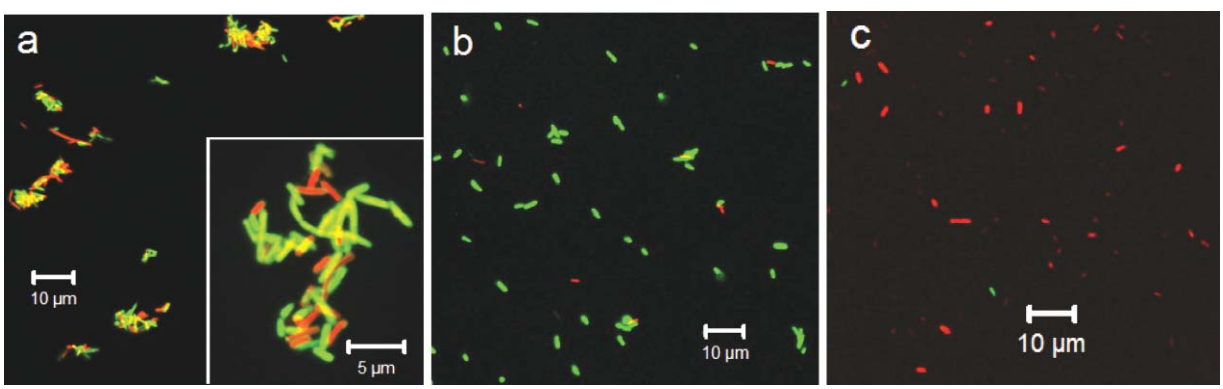

Fig. 4 Confocal microscopy images of PAO1 added to a solution of **3** (a) and **2** (b) in the dark. We note the formation of large bacterial clusters for **3** (a) with very few individual bacteria as compared to **2** (b) and to the live control (c). Red indicates live bacteria; green indicates dead bacteria. Live control is bacteria with same concentration but without beads or polymers.

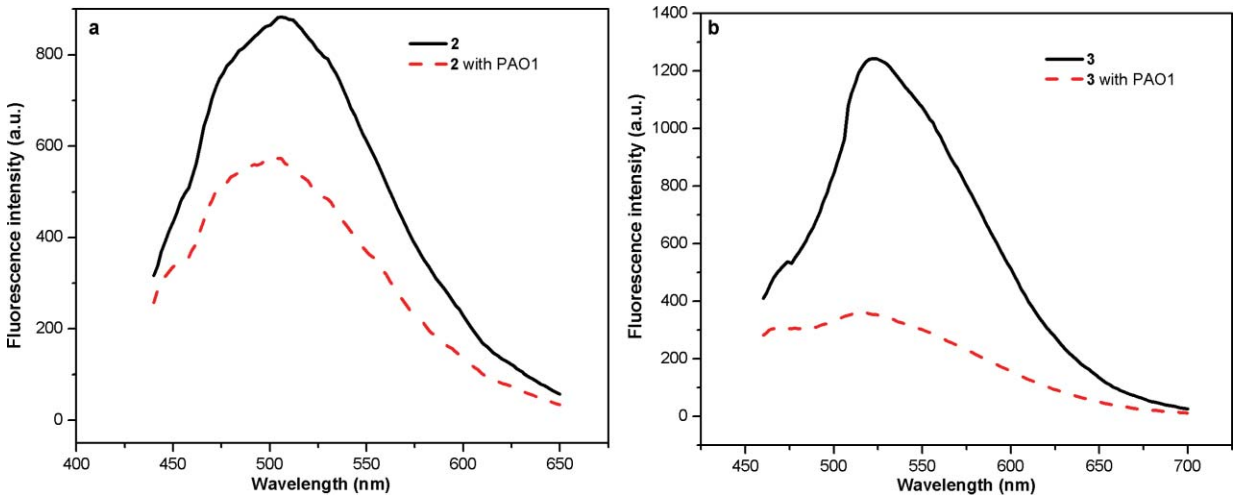

Fig. 5 Fluorescence spectra of polymer **2** (a, $\lambda_{ex} = 394$ nm) and **3** (b, $\lambda_{ex} = 427$ nm) with absence and presence of PAO1.

3.5 Singlet oxygen production

Our previous work demonstrates that cationic PPE-type CPEs sensitize singlet oxygen ($^1O_2$) due to triplet states generated by direct excitation of the CPEs.[23] In the present work, singlet oxygen sensitization by **2** and **3** was investigated in CD_3OD by monitoring the emission at 1260 nm. The $^1O_2$ emission intensity at 1260 nm was measured for various concentrations of the polymer in solution. A linear relationship was observed between the polymer absorbance at 335 nm and the $^1O_2$ emission intensity. The quantum yields of singlet oxygen generation were determined as 0.112 (± 0.008) for **3** and 0.122 (± 0.012) for **2** using 2′-acetonaphthone as an actinometer ($\Phi_\Delta = 0.79$).[35] The observation of the strong 1260 nm emission strongly supports the notion that these CPEs sensitize the production of $^1O_2$ in methanol solution.

Since the biocidal experiments were carried out in aqueous conditions, attempts were made to measure the quantum yields of $^1O_2$ emission sensitized by **3** and **2** in D_2O. However, the direct detection of $^1O_2$ emission was not possible in D_2O due to the very low efficiency of $^1O_2$ emission in this solvent.[23] Therefore, an indirect chemical method was utilized *via* chemical trapping of $^1O_2$ using the water soluble "chemical trapping agent" 1,3-cyclohexadiene-1,4-diethanoate (CHDDE). CHDDE reacts with $^1O_2$ to form stable peroxide (88%) and hydroperoxide (12%).[26] The reaction of CHDDE with $^1O_2$ is monitored by UV absorption spectroscopy. The disappearance of CHDDE is detected as decrease in its absorption band at 270 nm (Fig. 6). The quantum yield of $^1O_2$ production was determined according to the literature procedure using 5,10,15,20-tetrakis(4-sulfonatophenyl)porphyrin (TPPS) as an actinometer ($\Phi_\Delta = 0.66$) to give $\Phi_\Delta = 0.037$ for **3** and $\Phi_\Delta = 0.32$ for **2**.[23,36] These results clearly demonstrate that $^1O_2$ can be generated by irradiation of **2** or **3** in water. However, for **3**, the efficiency of $^1O_2$ generation in water is much lower than that in methanol. The decreased efficiency is consistent with the lower triplet yield of **3** in water due to quenching of singlet excited states by aggregation (*vide supra*). On the contrary, **2** generates singlet oxygen more efficiently in water than in methanol. Such a difference is most likely due to the high solubility of the polymer in water because of its high charge density per polymer repeat unit.

3.6 Influence of negatively charged phospholipids

A negatively charged phospholipid, DOPG, was chosen to interact with polymer **2** and **3** either in solution or on microspheres.

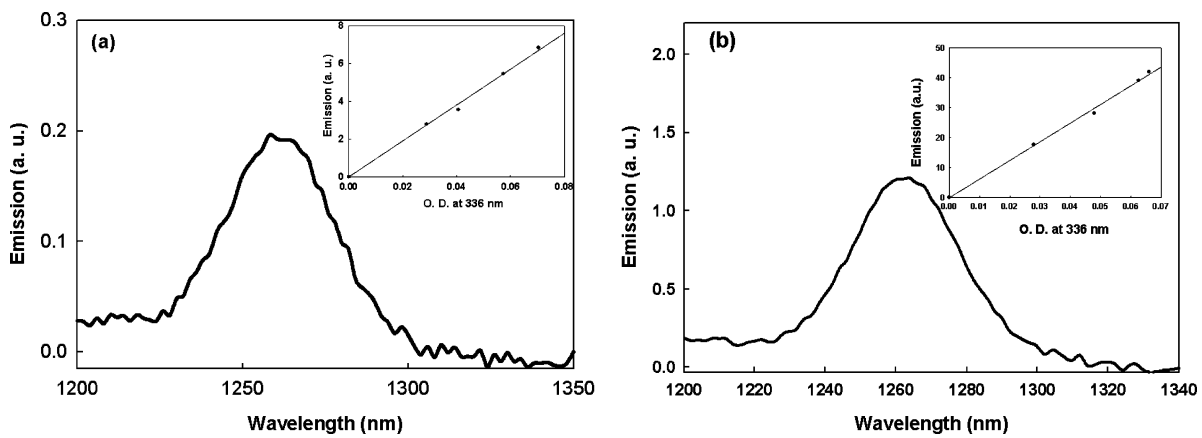

Fig. 6 Singlet oxygen emission sensitized by **3** (a) and **2** (b) in CD_3OD. Inset: Integrated $^1O_2$ emission intensity *versus* optical density of the polymer solution.

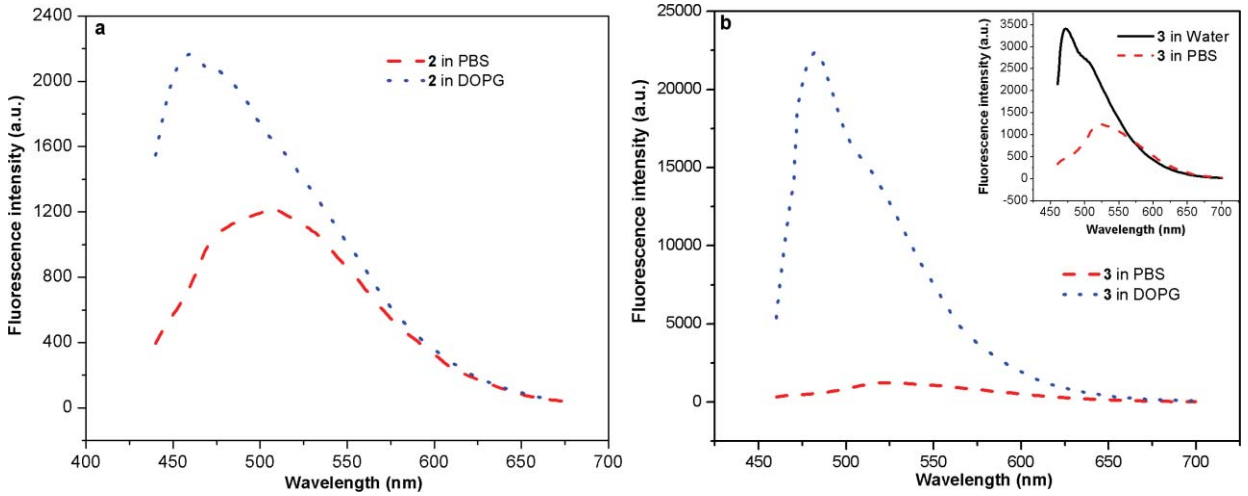

Fig. 7 Fluorescence spectra of polymers **2** (a, $\lambda_{ex} = 394$ nm) and **3** (b, $\lambda_{ex} = 427$ nm) in the absence and presence of DOPG liposomes.

The mixtures of polymer with DOPG liposome were prepared by adding 10 μL of stock PPE solutions to 1 mL of DOPG liposome solution followed by 30 min of vortexing. The resulting ratio between DOPG liposome and PPE polymer in repeat unit is 1 : 2000. (The hydrodynamic radius of DOPG liposomes prepared by the method mentioned earlier is *ca.* 110 nm as determined by dynamic light scattering.[37] This results in a calculated surface area of *ca.* 1.5×10^{-13} m^2 for each spherical liposome. As the surface area of each DOPG lipid is *ca.* 55×10^{-20} m^2, there are *ca.* 2.7×10^5 DOPG lipid in each DOPG liposome. Therefore, 1 mL of 2 mM of DOPG lipid solution can yield 7 nM of DOPG liposome. In 1 mL liposome–polymer mixtures, there are *ca.* 7×10^{-12} mol of DOPG liposome and *ca.* 1.3×10^{-8} mol of PPE repeat units, giving a ratio of 1 : 2000 between DOPG liposome and PPE repeat unit.) A control sample of polymer solution without DOPG liposome was also prepared by adding the same amount of polymer into 1 mL of PBS solution. Fig. 7 depicts the fluorescence spectra of polymers **2** and **3** in the presence and absence of DOPG liposome. Since DOPG was prepared in PBS buffer, the corresponding liposome-free samples of polymers were also measured in PBS buffer. For polymer **3**, its fluorescence emission in water was also measured and it was found that the change from water to PBS buffer induced a red shift from 475 nm to 524 nm. This showed that the increase in the ionic strength of the solvent makes the environment more hydrophilic and then resulted in more aggregation of polymer **3** and even weaker fluorescence emission. Interestingly, fluorescence enhancement and blue shifts of the emission maximum were found for both polymer **2** and **3** in the presence of DOPG, except that the extent of enhancement is different. In the case of polymer **2**, the emission maximum shifted from 506 nm to 460 nm and fluorescence intensity increased by less than 2 times in the presence of DOPG; on the other hand, in the case of polymer **3**, the emission maximum shifted from 524 nm to 482 nm and the fluorescence intensity increased by almost one order of magnitude. As described elsewhere and investigated in detail,[37] this fluorescence enhancement could be attributed to the interactions between cationic CPEs and negatively charged phospholipids, which induce association and further insertion of PPE CPs into DOPG liposome and results in some level of deaggregation of polymers and gives rise to increased fluorescence. The dramatic difference in the fluorescence enhancement between polymer **2** and **3** could be due to the difference in their structures, where **3** has a shorter and less sterically hindered pendant quaternary ammonium groups of **3** than **2**.

Similar results were also found for lipobeads, where a DOPG bilayer is coated on polymer **2** or **3** physisorbed microspheres. Although both blue shifts in the emission maximum and enhancement of fluorescence intensity were found for Si-**2**-DOPG and Si-**3**-DOPG, the fluorescence enhancement for Si-**3**-DOPG is dramatically larger than Si-**2**-DOPG, and there is about 7 times increase for the former, and less than 2 times for the latter.[37] This once again shows polymer **3** is easier to insert into the DOPG bilayer and provides for more efficient deaggregation. As a matter of fact, we discovered that polymer **3** showed fast and higher extent insertion into negatively charged phospholipid monolayer performed on Langmuir trough than polymer **2**.[37] Clearly polymer **3** is much more lipophilic than polymer **2** as indicated by the different interactions with negatively charged phospholipids. The enhanced lipophilicity of **3** is a reasonable source of the dark biocidal activity for polymer **3**.

4. Conclusion

In summary, we have found that polymer **3**, although similar in structure and overall photophysical behavior to the PPE polymers **1** and **2**, exhibits remarkable differences in its light activated and dark biocidal activity. Although at first surprising, the decrease in light-activated biocidal activity can be reasonably attributed to the aggregation of the polymer both in aqueous solution and physisorbed onto glass microspheres resulting in little or no production of singlet oxygen and reactive oxygen intermediates. The enhanced dark biocidal activity of **3** can be attributed to the increased lipophilicity of the polymer which may promote bacterial association while the quaternary ammonium functionality on the pendant ether side chains is likely responsible for the immediate cell killing.

Acknowledgements

This research is supported by the Defense Threat Reduction Agency (Contract No. W911NF-07-1-0079). Images in this manuscript were obtained using the confocal laser scanning microscope housed in the UNM/W.M. Keck Nanofluidics Laboratary.

References

1 E. R. Kenawy, S. D. Worley and R. Broughton, *Biomacromolecules*, 2007, **8**, 1359–1384.
2 R. Kugler, O. Bouloussa and F. Rondelez, *Microbiology*, 2005, **151**, 1341–1348.
3 L. Laopaiboon, S. J. Hall and R. N. Smith, *J. Appl. Microbiol.*, 2002, **93**, 1051–1058.
4 T. Thorsteinsson, M. Masson, K. G. Kristinsson, M. A. Hjalmarsdottir, H. Hilmarsson and T. Loftsson, *J. Med. Chem.*, 2003, **46**, 4173–4181.
5 J. C. Tiller, C. J. Liao, K. Lewis and A. M. Klibanov, *Proc. Natl. Acad. Sci. U. S. A.*, 2001, **98**, 5981–5985.
6 J. Y. Huang, R. R. Koepsel, H. Murata, W. Wu, S. B. Lee, T. Kowalewski, A. J. Russell and K. Matyjaszewski, *Langmuir*, 2008, **24**, 6785–6795.
7 A. Mecke, I. J. Majoros, A. K. Patri, J. R. Baker, M. M. B. Holl and B. G. Orr, *Langmuir*, 2005, **21**, 10348–10354.
8 M. R. Pinto and K. S. Schanze, *Synthesis*, 2002, 1293–1309.
9 B. Liu and G. C. Bazan, *Chem. Mater.*, 2004, **16**, 4467–4476.
10 K. E. Achyuthan, T. S. Bergstedt, L. Chen, R. M. Jones, S. Kumaraswamy, S. A. Kushon, K. D. Ley, D. McBranch, H. Mukundan, F. Rinisland, X. Shi, W. Xia and D. G. Whitten, *J. Mater. Chem.*, 2005, **15**, 2648–2656.
11 S. W. Thomas, G. D. Joly and T. M. Swager, *Chem. Rev.*, 2007, **107**, 1339–1386.
12 H. A. Ho, A. Najari and M. Leclerc, *Acc. Chem. Res.*, 2008, **41**, 168–178.
13 H. Jiang, P. Taranekar, J. R. Reynolds and K. S. Schanze, *Angew. Chem., Int. Ed.*, 2009, **48**, 4300–4316.
14 Q. Zhou and T. M. Swager, *J. Am. Chem. Soc.*, 1995, **117**, 12593–12602.
15 L. H. Chen, D. W. McBranch, H. L. Wang, R. Helgeson, F. Wudl and D. G. Whitten, *Proc. Natl. Acad. Sci. U. S. A.*, 1999, **96**, 12287–12292.
16 C. Y. Tan, M. R. Pinto and K. S. Schanze, *Chem. Commun.*, 2002, 446–447.
17 C. Y. Tan, E. Alas, J. G. Muller, M. R. Pinto, V. D. Kleiman and K. S. Schanze, *J. Am. Chem. Soc.*, 2004, **126**, 13685–13694.
18 D. T. McQuade, A. E. Pullen and T. M. Swager, *Chem. Rev.*, 2000, **100**, 2537–2574.
19 H. Jiang, X. Zhao, A. H. Shelton, S. H. Lee, J. R. Reynolds and K. S. Schanze, *ACS Appl. Mater. Interfaces*, 2009, **1**, 381–387.
20 P. Taranekar, Q. Qiao, H. Jiang, I. Ghiviriga, K. S. Schanze and J. R. Reynolds, *J. Am. Chem. Soc.*, 2007, **129**, 8958–8959.
21 L. D. Lu, F. H. Rininsland, S. K. Wittenburg, K. E. Achyuthan, D. W. McBranch and D. G. Whitten, *Langmuir*, 2005, **21**, 10154–10159.
22 T. S. Corbitt, J. R. Sommer, S. Chemburu, K. Ogawa, L. K. Ista, G. P. Lopez, D. G. Whitten and K. S. Schanze, *ACS Appl. Mater. Interfaces*, 2009, **1**, 48–52.
23 S. Chemburu, T. S. Corbitt, L. K. Ista, E. Ji, J. E. Fulghum, G. P. Lopez, K. Ogawa, K. S. Schanze and D. G. Whitten, *Langmuir*, 2008, **24**, 11053–11062.
24 X. Y. Zhao, M. R. Pinto, L. M. Hardison, J. Mwaura, J. Muller, H. Jiang, D. Witker, V. D. Kleiman, J. R. Reynolds and K. S. Schanze, *Macromolecules*, 2006, **39**, 6355–6366.
25 S. Chemburu, E. Ji, Y. Casana, Y. Wu, T. Buranda, K. S. Schanze, G. P. Lopez and D. G. Whitten, *J. Phys. Chem. B*, 2008, **112**, 14492–14499.
26 V. Nardello, N. Azaroual, I. Cervoise, G. Vermeersch and J. M. Aubry, *Tetrahedron*, 1996, **52**, 2031–2046.
27 Y. S. Wang and K. S. Schanze, *Chem. Phys.*, 1993, **176**, 305–319.
28 R. T. Farley, Ph.D. Dissertation, University of Florida, 2007.
29 R. Zeineldin, M. E. Piyasena, T. S. Bergstedt, L. A. Sklar, D. Whitten and G. P. Lopez, *Cytometry A*, 2006, **69a**, 335–341.
30 M. R. Pinto, B. M. Kristal and K. S. Schanze, *Langmuir*, 2003, **19**, 6523–6533.
31 K. Ogawa, S. Chemburu, G. P. Lopez, D. G. Whitten and K. S. Schanze, *Langmuir*, 2007, **23**, 4541–4548.
32 S. Senthilikumar, S. Nath and H. Pal, *Photochem. Photobiol.*, 2004, **80**, 104–111.
33 G. Jones, W. R. Jackson, C. Choi and W. R. Bergmark, *J. Phys. Chem.*, 1985, **89**, 294–300.
34 K. A. Walters, K. D. Ley and K. S. Schanze, *Chem. Commun.*, 1998, 1115–1116.
35 F. Wilkinson, W. P. Helman and A. B. Ross, *J. Phys. Chem. Ref. Data*, 1993, **22**, 113–262.
36 V. Nardello, D. Brault, P. Chavalle and J. M. Aubry, *J. Photochem. Photobiol., B*, 1997, **39**, 146–155.
37 L. Ding, unpublished result.